

36. P. S. Martin, R. G. Klein, Eds. *Quaternary Extinctions: A Prehistoric Revolution* (Univ. of Arizona Press, Tucson, AZ, 1984).
37. For financial support we thank the John D. and Catherine T. MacArthur Foundation and the NSF (DEB-9707281). We are grateful to Electrificación del Ca-

roni (EDELCA), the Venezuelan energy company that manages the Lago Guri impoundment, for authorizing the project and for numerous forms of logistical support. Many individuals assisted in the research and analysis of the data, and we acknowledge their indispensable roles: C. Aponte, A. R. Bruni, N. Cebal-

los, O. Cornejo, L. Davenport, P. Ferreyra, M. del C. Gomez, R. Hren, D. Koebbler, R. Leite, M. Potts, V. Salas, J. Tello, and L. Vergara. We thank two anonymous reviewers for their helpful comments.

27 July 2001; accepted 12 September 2001

Matching Spiracle Opening to Metabolic Need During Flight in *Drosophila*

Fritz-Olaf Lehmann

The respiratory exchange system of insects must maximize the flux of respiratory gases through the spiracles of the tracheal system while minimizing water loss. This trade-off between gas exchange and water loss becomes crucial when locomotor activity is increased during flight and metabolic needs are greatest. Insects that keep their spiracles mostly closed during flight reduce water loss but limit the flux of oxygen and carbon dioxide into and out of the tracheal system and thus attenuate locomotor performance. Insects that keep their spiracles completely open allow maximum gas exchange but face desiccation stress more quickly. Experiments in which water vapor was used as a tracer gas to track changes in the conductance of the respiratory system indicated that flying fruit flies minimize potential water loss by matching the area of the open spiracles to their gas exchange required for metabolic needs. This behavior maintained approximately constant pressure for carbon dioxide (1.35 kilopascals) and oxygen (19.9 kilopascals) within the tracheal system while reducing respirometric water loss by up to 23% compared with a strategy in which the spiracles are held wide open during flight. The adaptive spiracle-closing behavior in fruit flies has general implications for the ecology of flying insects because it shows how these animals may cope with environmental challenges during high locomotor performance.

The increased power output required for flapping flight places special demands and constraints on the respiratory system of flying insects (1). On the one hand, the respiratory system must permit the flux of oxygen (O_2) and carbon dioxide (CO_2) to and from flight muscles. On the other hand, the structures that permit respiratory exchange leave an animal susceptible to the loss of water vapor, thus increasing the danger of desiccation. The spiracles that occlude the outer openings of the insect tracheal system function as barriers that control the gas exchange between the network of air sacs, tracheas, and tracheoles and the outer environment. The terminal internal endings of the tracheal system, the tracheoles, are thought to be water filled, establishing a pressure that continuously drives water vapor out of the insect body when spiracles open for gas exchange (2–5). The potential threat of desiccation is greatest during flight, when the spiracles must remain open to sustain increased metabolic activity of the wing muscles. The metabolic cost of

flight is not constant, however, but varies as an animal alters force production to carry loads or perform flight maneuvers (6–8).

In a diffusion-based respiratory system (9), the rate with which a gas is exchanged depends on two factors: the partial-pressure

gradient between ambient and tracheal gas, and the cross-sectional area for diffusive flux (the area of the spiracle opening). The driving force on water vapor is assumed to be constant, so the flux of water depends only on the size of spiracle opening (10). The situation for the respiratory gases (CO_2 and O_2) is more complex, because the internal tracheal partial pressures might vary with metabolic rate. To limit water loss, an insect ought to match spiracle opening with its instantaneous metabolic demands. To test this hypothesis, I developed a method for indirectly measuring spiracle-opening area in tethered fruit flies, *Drosophila melanogaster*, flying within a respirometric chamber of a virtual-reality flight arena and estimated the concomitant changes in partial pressure of tracheal gases from simultaneous measurements of total flight force production, CO_2 release, and water-loss rate (11, 12). The experiments were performed under visual closed-loop feedback conditions, in which the fly itself controls the angular velocity of a vertical dark stripe displayed in the arena by changing the stroke amplitude of its two wings during flight. Under these conditions, a fruit fly attempts to stabilize the azimuth position of the dark stripe in the frontal region of its visual field. While the animal actively controlled the dark bar, a superimposed background pattern of diagonal stripes was oscillated vertically around the animal.

In the fruit fly, 4 thoracic and 14 abdominal spiracles control the diffusive flux into

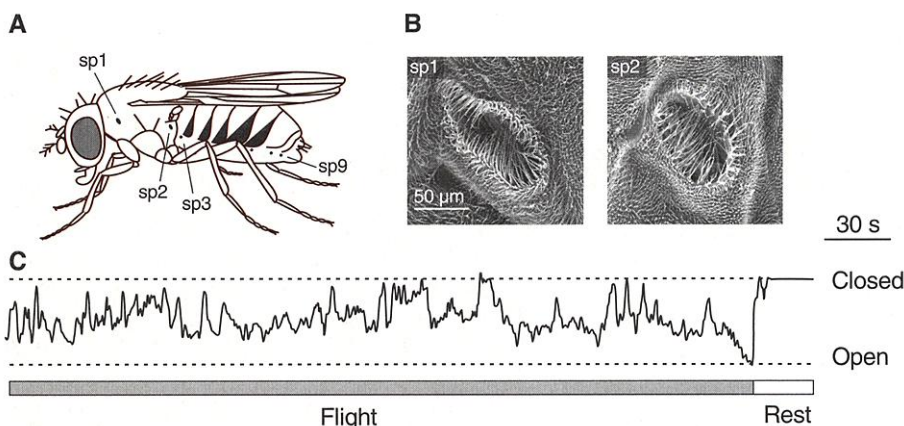


Fig. 1. Location of spiracle openings, and spiracle closing and opening behavior during flight, in the fruit fly *Drosophila*. (A) sp1, mesothoracic spiracle; sp2, metathoracic spiracle; sp3 to sp9, abdominal spiracles. (B) The oval thoracic spiracular openings are bordered by a thick sclerite and protected with hairs. Narrow flexible spiracular lids cover the tracheal entrance. Spiracles open by the elasticity of their cuticular structures and are held actively closed by the spiracle-closing muscle (32). Images are taken from *D. virilis*. (C) Closing and opening behavior of the right mesothoracic spiracle in *D. mimica* Hardy (3.06 mg wet body mass) during tethered flight and rest (33).

Theodor-Boveri-Institute, Department of Behavioral Physiology and Sociobiology, University of Würzburg, Am Hubland, 97074 Würzburg, Germany. E-mail: lehmann@biozentrum.uni-wuerzburg.de

REPORTS

and out of the tracheal system (Fig. 1, A and B). Although it is possible to record directly the mesothoracic spiracle opening area in flight of the large Hawaiian species *D. mimica* by video microscopy (Fig. 1C), it is difficult to monitor the opening and closing

of all spiracles simultaneously during flight in smaller species of *Drosophila*. The beating haltere, moreover, partly blocks the view on the opening of the large metathoracic spiracle. In addition, the small tracheole endings in fruit flies are inaccessible for direct pres-

sure measurements of respiratory gases. I thus derived the average opening behavior of all 18 spiracles and the average partial pressure for tracheal CO₂ and O₂ during flight by estimating the conductance for tracheal gas flux from the measured water-loss rates of the fly.

The tracheal partial pressure of CO₂ and O₂ may be expressed by using a geometric model for tracheal diffusion (13) in which the respirometric flux of a gas through the spiracles, \dot{M} , is the product of conductance for diffusion, G , and the driving force given by the difference of tracheal partial pressure, P_T , and partial pressure in the ambient air, P_A :

$$P_T = \dot{M}G^{-1} + P_A \quad (1)$$

During flight, the conductance for CO₂ and O₂ is expected to vary with the changes in the open area of the spiracles. If certain assumptions are met, mean conductance for respirometric gas flux within a short period of time (100 ms) can be derived from the conductance of water vapor because both gases follow the same diffusive path. Assuming that the water-filled tracheole ends establish a constant driving force, conductance for water was derived from the measured water flux according to Eq. 1 (14). The functional geometry of the tracheal system is given by the relation

$$A_T L_T^{-1} = GD^{-1}\beta^{-1} \quad (2)$$

in which A_T is the representative cross-sectional area and L_T the characteristic length of the tracheal system, D is the effective diffusion coefficient of the gas, and β is the capacitance coefficient. Given these geometric parameters, the conductance for CO₂ and O₂ within the tracheal system may then be estimated by replacing D and β in Eq. 2 with values appropriate for CO₂ and O₂ (15, 16). Assuming that maximum tracheal conductance matches the need for respiratory gas exchange at maximum locomotor performance, the total opening area of all spiracles, A_S , can be approximated by setting maximum total spiracle area, A_{\max} , of 5949 μm^2 (17) equal to the extreme 1% of all values of A_T within a flight sequence in which metabolic needs are the greatest. Overall opening area in the flying insect may be eventually calculated by

$$A_S = A_T L_T^{-1} A_{\max} (A_T L_T^{-1})_{\max}^{-1} \quad (3)$$

Tethered flying fruit flies typically modulated their total flight force production in response to the vertical oscillating diagonal stripe pattern in an attempt to minimize the slip of the retinal image (Fig. 2A, green and black traces). In freely flying flies this optomotor behavior would stabilize the vertical position of the animal in space. The modulation of flight force was accompanied by regular changes of both CO₂ release and respiratory water loss (Fig. 2A, red and blue traces). While the fly

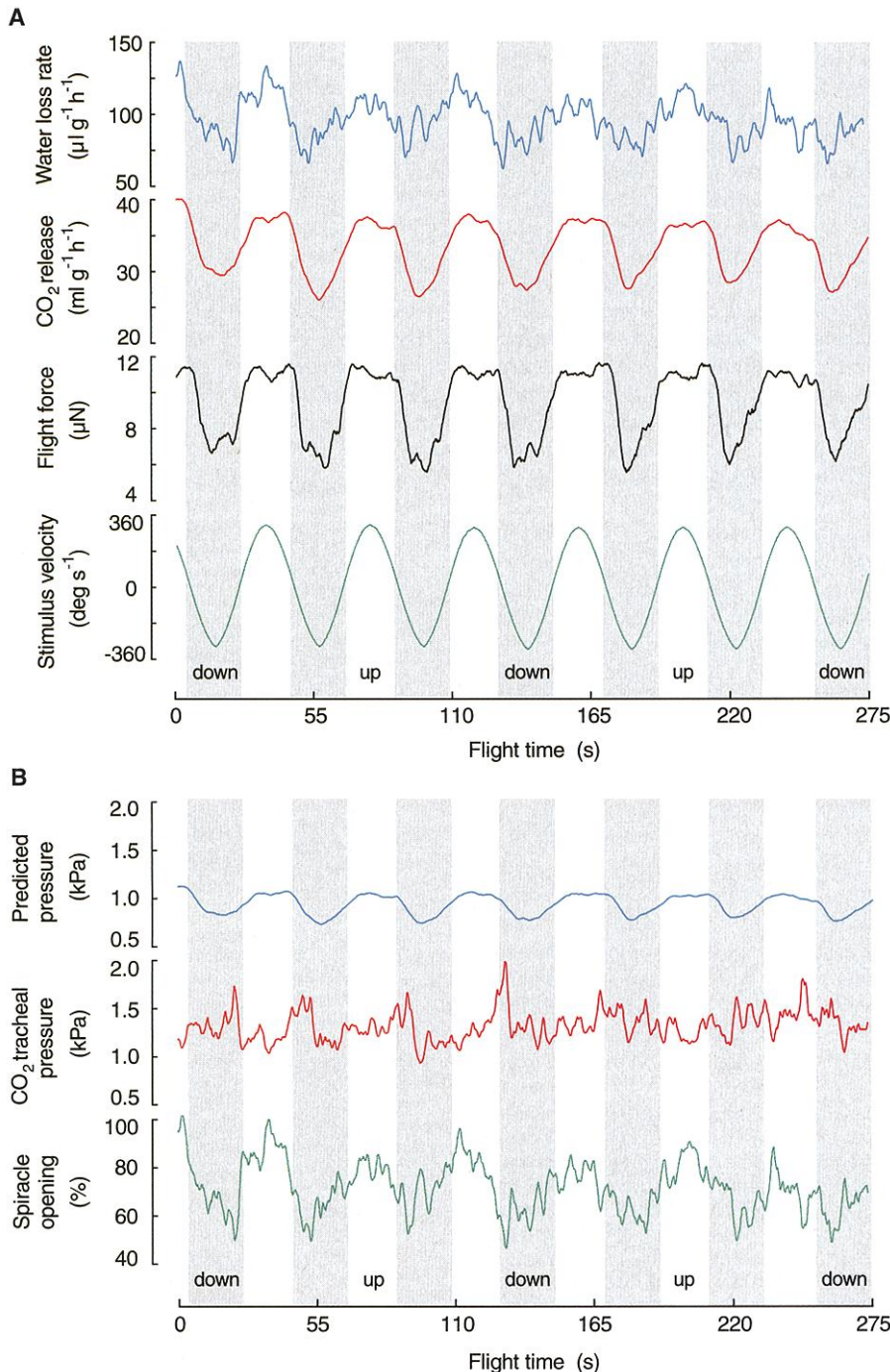


Fig. 2. Alterations in flight performance and concomitant changes in respiratory behavior of a single *D. melanogaster* fruit fly. (A) Representative recording showing water-loss rate (blue) and CO₂ release (red) while the tethered animal varied its flight force (black) in response to the vertical motion of a stripe pattern (green) displayed in the flight arena. Negative angular velocities of the visual stimulus indicate that the stripe pattern moves downwards (gray areas). Both respirometric values are given in units that take into account the body mass of the fly. (B) Spiracle-opening behavior (green) and tracheal partial pressure for CO₂ (red) in flying flies were determined with a geometric model for tracheal diffusion. Assuming that spiracles are held continuously open during flight, tracheal partial pressure would vary in-phase with flight-power requirements (blue).

was responding to the motion of the moving pattern, CO_2 flux varied by $35 \pm 11\%$ of its mean value, which reflected the changes in energy expenditures during flight (Table 1). The modulation of water loss rate by $26 \pm 14\%$ indicates either that (i) *Drosophila* does not hold its spiracles continuously open during flight as reported in previous studies on large beetles (18); (ii) an increase in strain amplitude of the asynchronous flight power muscles intensifies thoracic autoventilation and thus enhances water loss in proportion to flight force production; or (iii) changes in

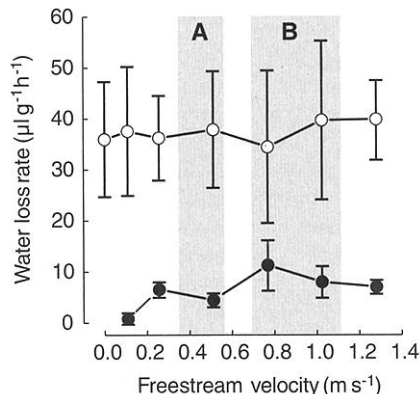


Fig. 3. Total water-loss rate (○) and cuticle water loss (●) in unrestrained *D. melanogaster* plotted against free-stream velocity of the ambient air. A total of 114 flies were exposed for 4 hours to different flow velocities of dry air within a small respirometric chamber in which water-loss rate and CO_2 release were simultaneously measured by flow-through respirometry. Total water-loss rate was determined from weight loss. To yield cuticle water-loss rates, spikes of water loss due to discontinuous gas exchange, droplets, and proboscis extensions were estimated by flow-through respirometry and then subtracted from total loss. The gray areas represent the expected ranges of induced mean air velocity produced by the beating wings during flight (A) near the stroke plane and (B) in the "far" wake behind the animal, while the fly modulates its aerodynamic forces between minimum and maximum values (19).

Table 1. Alterations in flight performance, gas-exchange rates, spiracle activity, and partial pressure of CO_2 and O_2 with maximal and minimal power output. Modulation was defined as the ratio between the difference and half the sum of maximum and minimum performance. Force, total flight force production; $\dot{V}^*\text{CO}_2$, flight-specific flux of CO_2 through spiracles; $\dot{V}^*\text{H}_2\text{O}$, flight-specific rate of water loss; A_s , total spiracle opening area; P_{T,CO_2} , tracheal partial pressure for CO_2 ; P_{P,CO_2} , predicted tracheal partial pressure for CO_2 based on the assumption that the spiracles are held continuously open during flight; and P_{T,O_2} , partial pressure for tracheal O_2 . The data were collected from 13 females. Two flight sequences were typically recorded from each animal, representing a mean flight time of 13 ± 6 min. Mean body mass of the animals = 1.05 ± 0.13 mg. All values shown are the means \pm SD.

Force (μN)	$\dot{V}^*\text{CO}_2$ ($\text{ml g}^{-1} \text{hour}^{-1}$)	$\dot{V}^*\text{H}_2\text{O}$ ($\mu\text{l g}^{-1} \text{hour}^{-1}$)	A_s (μm^2)	P_{T,CO_2} (kPa)	P_{P,CO_2} (kPa)	P_{T,O_2} (kPa)
<i>Maximum performance</i>						
13.0 ± 1.7	39 ± 4.2	104 ± 16	5949	1.4 ± 0.2	1.4 ± 0.2	19.8 ± 0.2
<i>Minimum performance</i>						
5.1 ± 1.3	27 ± 3.4	81 ± 18	4606 \pm 648	1.3 ± 0.2	1.0 ± 0.2	19.9 ± 0.2
<i>Modulation (%)</i>						
88 ± 17	35 ± 11	26 ± 14	26 ± 14	11 ± 7.7	35 ± 11	0.6 ± 0.3

wing kinematics modulate induced air-flow velocity (19), which in turn alters cuticle water-loss rate due to changes in the boundary-layer condition around the animal. Experiments in which cuticle water-loss rates were determined in unrestrained flies, however, reveal that mean cuticle water-loss rate is relatively low ($6.4 \pm 1.4 \mu\text{l g}^{-1}$ body mass hour^{-1}) and did not significantly increase with increasing flow velocity of the ambient air over a wide range of different values (linear regression, t test on slope, $P > 0.2$) (Fig. 3). It thus seems unlikely that changes of water-loss rate during flight are due to alterations in cuticle water loss. The same holds for possible alterations in thoracic autoventilation of the tracheal system because the oscillations in length of the thoracic box in *Drosophila* range only between 2 and 5% throughout a complete contraction-extension cycle of the flight muscles (20). Moreover, in small insects such as fruit flies, thoracic autoventilation and tracheal ventilation due to the Bernoulli effect (18) are thought to be greatly attenuated by the low Reynolds number for tracheal air flow (21).

Instead, in response to a drop in flight power requirements, fruit flies appear to actively reduce average opening area of all 18 spiracles by up to $77 \pm 11\%$ of their maximum area. At a flight force that is equal to body weight, the flux of water is reduced by $11.6 \pm 5.6\%$ or $12.1 \pm 5.8 \mu\text{l g}^{-1}$ body mass hour^{-1} compared with the maximum value. Although the fly is modulating flight force production by $88 \pm 17\%$, tracheal partial pressure for CO_2 and O_2 as calculated from Eq. 1 appear not to be correlated with flight force production or metabolic rate, yielding means of 1.35 ± 0.16 and 19.9 ± 0.16 kPa, respectively (Fig. 2, A and B). These results are consistent with the hypothesis that *Drosophila* limits water loss during flight by actively matching the extent of spiracle opening to its metabolic needs (22, 23). Moreover, the high partial pressure for tracheal oxygen

strongly supports the assumption that diffusion alone can account for gas exchange during flight in fruit flies (24).

In contrast to findings in other insects, this study shows that fruit flies appear to control the diffusive flux for respiratory gases through their spiracles by modulating the opening area of the spiracles. This modulation in mean cross-sectional area of the diffusive path results in nearly constant mean partial pressure for CO_2 and O_2 in the tracheal system, even though metabolic demands vary substantially during flight. Although this finding may not explain the mechanism whereby each spiracle contributes to overall tracheal conductance during flight (25), it demonstrates how small insects may cope with environmental challenges during increased locomotor performance. By whatever mechanism, in the diffusion-based respiratory system of *Drosophila*, the adaptive spiracle-closing behavior should lower the risk of desiccation for animals flying under dry environmental conditions.

References and Notes

- C. P. Ellington, *J. Exp. Biol.* **160**, 71 (1991).
- J. W. L. Beament, *Adv. Insect Physiol.* **2**, 67 (1964).
- E. B. Edney, *Water Balance in Land Arthropods* (Springer-Verlag, New York, 1977).
- V. B. Wigglesworth, *Adv. Insect Physiol.* **17**, 85 (1983).
- Wigglesworth (4) argued that during muscular activity, the fluid might be removed from the tracheoles in some insects. In flying fruit flies, however, I found that flight-specific water-loss rates do not tend to decrease within flight sequences lasting up to 1 hour.
- J. Marden, *J. Exp. Biol.* **130**, 235 (1987).
- F.-O. Lehmann, M. H. Dickinson, *J. Exp. Biol.* **200**, 1133 (1997).
- F.-O. Lehmann, *J. Comp. Physiol. B* **169**, 165 (1999).
- Although small insects like *Drosophila* are thought to rely on diffusion, the dorsal air sacs pulse rhythmically during flight due to the work of the contractions of the aorta and accessory organs. However, these changes in pressure within tracheal system seem to be of little functional importance, and there is almost no net change in thoracic volume (24).
- J. R. B. Lighton, D. A. Garrigan, F. D. Duncan, R. A. Johnson, *J. Exp. Biol.* **179**, 233 (1993).
- Under steady-state metabolic conditions, the flux of O_2 can be estimated from the measured CO_2 release through the spiracles. Within diptera, glycogen is the primary source of fuel during flight, yielding a respiratory quotient of 1.0 (26). Because the insect flight muscle is thought to have almost no anaerobic capacity, the flux of O_2 into the tracheal system must be roughly equal to the measured flux of CO_2 out of the system.
- Cold-anesthetized animals were glued to a tungsten holder by means of ultraviolet light-curing adhesive and aligned in an 18-ml flow-through respirometric chamber. Water and CO_2 were removed from room air, which was pulled through the chamber at a flow rate of 200 ml min^{-1} , regulated by a mass flow controller, and then analyzed in a gas analyzer (average time 100 ms) at 24°C ambient temperature. Resting values recorded before and after each flight sequence were subtracted from the raw signal to yield flight-specific rates of water loss and CO_2 release. In *D. melanogaster*, the elevation of the total mean flight force vector is always orientated at an angle of 24° with respect to the horizontal body axis and does not vary with the animal's absolute orientation in space. This relation was used to reconstruct total flight force from the measured force component parallel to the body axis by using a microlaser balance (7).

13. P. Kestler, in *Environmental Physiology and Biochemistry of Insects*, K. H. Hoffmann, Ed. (Springer-Verlag, Berlin, 1985), pp. 137–186.
14. Because water and CO₂ were removed from room air, the ambient partial pressure for CO₂ and water vapor was close to zero within the respirometric chamber. Pressure measurements inside the chamber yielded normal barometric pressure, and thus ambient partial pressure for O₂ amounted to ~20.95 kPa. Partial pressure for saturated water vapor is 3.29 kPa measured at 25°C (27).
15. The effective diffusion coefficient in air is 0.165 cm² s⁻¹ (for CO₂), 0.209 cm² s⁻¹ (for O₂), and 0.251 cm² s⁻¹ (for water vapor) at 25°C (28). The capacitance coefficient of CO₂, O₂, and water vapor in air is 410.5 nmol cm⁻³ kPa⁻¹ measured at a pressure of 101.3 kPa and at 20°C (13).
16. The characteristic length and thus the point in the tracheal system at which internal partial pressure estimates apply was approximated at maximum water-loss rate and assuming that all spiracles are completely open. Equation 2 then yields a characteristic length of about 111 ± 14 μm (mean ± SD). The thorax width of *D. melanogaster* is ~0.8 mm.
17. G. Manning, M. A. Krasnow, in *The Development of Drosophila melanogaster*, M. Bate, A. M. Arias, Eds. (Cold Spring Harbor Laboratory Press, Cold Spring Harbor, NY, 1993), pp. 609–686.
18. P. L. Miller, *J. Exp. Biol.* **45**, 285 (1966).
19. Mean induced air velocity in the wake behind the two beating wings was estimated from the Rankine-Froude axial momentum theory that determines the air velocity from the momentum flux of air required to provide a given flight force. In the simplest case the wake is considered as a steady-state jet through an actuator disk with a uniform distribution of air velocities. Mean induced velocity, w_0 , close to the stroke plane is given by the equation $w_0 = \left(\frac{1}{2} F \rho^{-1} A_0^{-1}\right)^{0.5}$, in which F is total flight force, ρ is the density of the air, and A_0 is the area swept by the two beating wings. Due to wake constriction, the theory shows that in the “far” wake the active area is solely $\frac{1}{2} A_0$ whereas induced velocity reaches $2w_0$ (29). Direct measurements of induced air velocity in the wake behind tethered flying fruit flies that responded to optomotor lift stimuli showed alterations in peak air velocity ranging from 0.88 at low flight forces to 0.94 m s⁻¹ at maximum force production (30).
20. W. P. Chan, M. H. Dickinson, *J. Exp. Biol.* **199**, 2767 (1996).
21. The Reynolds number (Re) for tracheal air flow was approximated with a conventional model for flow in pipes that is given by $Re = u d \nu^{-1}$ (28). In this equation u is flow velocity, d is the pipe diameter, and ν is the kinematic viscosity of air. To derive an upper estimate of Re , I assumed Bernoulli ventilation of the tracheas at maximum induced air-flow velocity of 0.94 m s⁻¹ (29). The tracheal diameter was set to the maximum opening area of the large thoracic spiracles of ~42.5 μm. At a kinematic viscosity for air of 15×10^{-6} m² s⁻¹ (20°C), Re for tracheal air flow is about 2.7.
22. In *D. melanogaster*, the four thoracic spiracles form oval openings at the surface of about 60 μm by 25 μm each, whereas the circular openings of the 14 smaller abdominal spiracles are about 5 μm in diameter (17). From these values I calculated a total cross-sectional area of thoracic and abdominal openings of 5675 and 275 μm², respectively. Assuming that only thoracic spiracles contribute to respiratory gas exchange, the given estimates for internal partial gas pressure would slightly change by ~5%.
23. Direct recordings of oxygen partial pressure in the flight muscle of large sweetpotato hawkmoths *Agrius convolvuli* made with microelectrodes have shown that internal oxygen concentration remains constant during the transition from rest to flight (31). Although large moths probably primarily use variation in tracheal convection to achieve stable internal partial pressure of respiratory gases, the finding suggests that constant partial pressure for oxygen might be preserved across even disparate insect species.
24. T. Weis-Fogh, *J. Exp. Biol.* **41**, 229 (1964).
25. The derived measures for overall tracheal conductance, internal partial gas pressure, and mean

opening area of the spiracles appear to be consistent with at least three different basic mechanisms of spiracle control. The fly may achieve an average tracheal conductance either by (i) matching the opening area of each spiracle to the respiratory needs, (ii) closing some spiracles while other spiracles remain open, or (iii) dynamically closing and opening the spiracles over time. Although all mechanisms could give similar mean tracheal conductance within the 100-ms time period used by the gas analyzer, periodically closing spiracles might increase the variance of tracheal partial pressures at a given flight force. Moreover, assuming that the spiracles ensure rather homogenous levels of oxygen throughout the active flight-muscle tissue, it seems unlikely that some thoracic spiracles are completely closed whereas others are completely open during flight.

26. R. Ziegler, in *Environmental Physiology and Biochemistry of Insects*, K. H. Hoffmann, Ed. (Springer-Verlag Berlin, 1985), pp. 95–118.
27. C. Gerthsen, H. Vogel, *Physik* (Springer-Verlag, Berlin, 1993), p. 238.
28. M. W. Denny, *Air and Water: The Biology and Physics*

of *Life's Media* (Princeton Univ. Press, Princeton, NJ, 1993), pp. 70–89.

29. C. P. Ellington, *Philos. Trans. R. Soc. London Ser. B* **305**, 115 (1984).
30. F.-O. Lehmann, thesis, University of Tübingen, Germany (1994).
31. Y. Komai, *J. Exp. Biol.* **201**, 2359 (1998).
32. T. B. Nikam, V. V. Khole, *Insect Spiracular Systems* (Halsted, New York, 1989).
33. Real-time fractional opening of the mesothoracic spiracle during flight was derived from intensity changes of light that was focused on the spiracle entrance by using small fiber optics. The amount of light reflected by the moving spiracular lids and thus the brightness of the spiracle's video image was greatest when the lids completely covered the spiracle entrance. Video images for calibration and data analysis were taken at 60-Hz sampling frequency with a conventional video camera.
34. I thank M. H. Dickinson for reading an early version of this manuscript. Supported by grants from the German Science Foundation (Le-905/4) and BMBF (BioFuture 0311885).

27 July 2001; accepted 23 October 2001

Real-Time Single-Molecule Imaging of the Infection Pathway of an Adeno-Associated Virus

Georg Seisenberger,¹ Martin U. Ried,² Thomas Endreß,¹ Hildegard Büning,² Michael Hallek,^{2,3} Christoph Bräuchle^{1*}

We describe a method, based on single-molecule imaging, that allows the real-time visualization of the infection pathway of single viruses in living cells, each labeled with only one fluorescent dye molecule. The tracking of single viruses removes ensemble averaging. Diffusion trajectories with high spatial and time resolution show various modes of motion of adeno-associated viruses (AAV) during their infection pathway into living HeLa cells: (i) consecutive virus touching at the cell surface and fast endocytosis; (ii) free and anomalous diffusion of the endosome and the virus in the cytoplasm and the nucleus; and (iii) directed motion by motor proteins in the cytoplasm and in nuclear tubular structures. The real-time visualization of the infection pathway of single AAVs shows a much faster infection than was generally observed so far.

Single-molecule detection techniques have been developed for imaging and for spectroscopic characterization of individual fluorescent molecules (1–3). Within the last years, these techniques have been increasingly applied to biological topics (4, 5). By overcoming the problem of ensemble averaging, these techniques enabled questions in molecular biology to be solved, which hitherto could not be an-

swered by conventional ensemble measurements (6–8). Single-molecule imaging has previously been applied to study the diffusional behavior of single molecules in lipid bilayers (9, 10), in fluids (11–13), or recently, in living cells (14) and their membranes (15, 16). Here, we show for the first time that this method can be used for the visualization and kinetic characterization of the infection pathway of single viruses in living cells.

The viral infection process is a very intriguing interaction in nature. It starts with the contact between the virus and the cell membrane and finally results in transport of the virus into the nucleus and gene expression. For antiviral drug design, as well as for the development of efficient gene therapy vectors, it is essential to understand these processes. Electron microscopy is one tool for obtaining knowledge on the

¹Department Chemie, Ludwig-Maximilians-Universität München, Butenandtstraße 11, D-81377 München, Germany. ²Genzentrum, Laboratorium für Molekulare Biologie, Medizinische Klinik III, Klinikum Großhadern, Ludwig-Maximilians-Universität München, Feodor-Lynen-Straße 25, D-81377 München, Germany. ³GSF—National Center for Research and Environment, KKG Gentherapie, Marchioninistraße 25, D-81377, Germany.

*To whom correspondence should be addressed. E-mail: christoph.braeuchle@cup.uni-muenchen.de